α-Cyclodextrin Host–Guest Binding: A Computational Study of the Different Driving Forces

by **Sereina Riniker**[a]), **Xavier Daura**[b]), and **Wilfred F. van Gunsteren***[a])

[a]) Laboratory of Physical Chemistry, Swiss Federal Institute of Technology, ETH, CH-8093 Zürich (phone: +41-44-6325501; e-mail: wfvgn@igc.phys.chem.ethz.ch)

[b]) Catalan Institution for Research and Advanced Studies (ICREA) and Institute of Biotechnology and Biomedicine (IBB), Universitat Autònoma de Barcelona, ES-08193 Bellaterra, Barcelona

Free-energy differences govern the equilibrium between bound and unbound states of a host and its guest molecules. The understanding of the underlying entropic and enthalpic contributions, and their complex interplay are crucial for the design of new drugs and inhibitors. In this study, molecular dynamics (MD) simulations were performed with inclusion complexes of α-cyclodextrin (αCD) and three monosubstituted benzene derivatives to investigate host–guest binding. αCD Complexes are an ideal model system, which is experimentally and computationally well-known. Thermodynamic integration (TI) simulations were carried out under various conditions for the free ligands in solution and bound to αCD. The two possible orientations of the ligand inside the cavity were investigated. Agreement with experimental data was only found for the more stable orientation, where the substituent resides inside the cavity. The better stability of this conformation results from stronger *Van der Waals* interactions and a favorable antiparallel host–guest dipole–dipole alignment. To estimate the entropic contributions, simulations were performed at three different temperatures (250, 300, and 350 K) and using positional restraints for the host. The system was found to be insensitive to both factors, due to the large and symmetric cavity of αCD, and the nondirectional nature of the host–guest interactions.

Introduction. – α-Cyclodextrin (αCD) belongs to a family of cyclically closed oligosaccharides linked by α-bonds, where the number of glucose units ranges from six (αCD) to eight (γCD). The central cone-shaped cavity of cyclodextrins has hydrophobic character relative to bulk water, although actually semipolar [1][2], while the rims of the cavity are hydrophilic due to the OH groups of glucose. The ability of αCD to bind small organic compounds in this cavity together with its small size renders it an ideal model for computational studies of host–guest binding [3–5]. In addition, the system is well-studied experimentally [2][6–12]. Molecular dynamics (MD) simulations have reproduced the experimental relative free energies of binding [3]. These free-energy differences are a complex interplay of enthalpic and entropic contributions; however, the main driving force of complexation has not been identified yet. Possible effects are changes in *Van der Waals* forces [10][13], hydrophobic interactions [14], and dipole–dipole alignment [10][15], as well as electronic repulsion between frontier orbitals [16] (for an overview, see [12]). *Liu* and *Guo* [10] and *Estrada et al.* [16] found the electronic effects to be more important in αCD inclusion complexes, whereas *Cai et al.* [13] concluded that *Van der Waals* interactions are the most decisive ones. In addition, guest orientation in the cavity, steric effects, and the flexibility of the host may affect the equilibrium of the system. As the relative contributions of the

different driving forces mentioned above cannot be determined experimentally, MD simulations can give additional insight. Here, we provide, as complement to experiment, an analysis of these various factors for three ligands.

Computational Methods. – *Computation of Relative Free Energies and Entropies.* For the calculation of the free-energy difference ΔG_{BA} between two states A and B, only the regions of phase space that are relevant to the transition from state A to B must be sampled. There are various approaches to estimate ΔG_{BA} from MD simulations, wherein thermodynamic integration (TI) [17] is one of the most accurate methods. Applying TI, the system is changed stepwise, under the control of a coupling parameter λ, from state A ($\lambda = 0$) to state B ($\lambda = 1$). This change involves changing the character and interactions, *i.e.*, force field parameters, of a small set of atoms from their value in state A to those in state B [18]. In the present case, the λ-dependence of the potential energy of the system is specified in [19–21]. The free-energy difference ΔG_{BA} is then given by *Eqn 1*.

$$\Delta G_{BA} = G(\lambda_B) - G(\lambda_A) = \int_{\lambda_A}^{\lambda_B} \left\langle \frac{\partial V(\lambda)}{\partial \lambda} \right\rangle_{\lambda} d\lambda \tag{1}$$

ΔG_{BA} is obtained by performing a finite number (N_λ) of simulations at discrete λ values ranging from 0 to 1 and subsequent numerical integration using interpolation formulae. Thus, given sufficiently long simulations, the system is at each λ value at equilibrium. Compared to free-energy differences, the estimation of relative entropies requires more extensive sampling of the phase space. There are different approaches to reduce the sampling problem, providing estimates with varying degree of accuracy. The possibly most accurate method [22] is based on a finite temperature difference using the relation $S = -\left(\frac{\partial G}{\partial T}\right)_{Np}$, where ΔS_{BA} can be expressed as

$$\Delta S_{BA} = -\frac{\Delta G_{BA}^{TI}(T + \Delta T) - \Delta G_{BA}^{TI}(T - \Delta T)}{2\Delta T} \tag{2}$$

Computation of Relative Free Energies of Binding. Free energy of binding $\Delta G_{binding}$ is the free-energy difference between the bound and the unbound state for a specific ligand, and can be derived using the experimentally available binding constant K_i and the relation

$$\Delta G_{binding} = -RT \ln(K_i) \tag{3}$$

As these $\Delta G_{binding}$ values are computationally inaccessible with unbiased computational methods, only the relative binding free energies $\Delta\Delta G_{binding}^{BA}$ between two ligands A and B can be compared. Making use of a thermodynamic cycle, one finds

$$\Delta\Delta G_{binding}^{BA} = \Delta G_{binding}^{B} - \Delta G_{binding}^{A} = \Delta G_{BA}^{bound} - \Delta G_{BA}^{unbound} \tag{4}$$

where $\Delta G^{A}_{binding}$ and $\Delta G^{B}_{binding}$ are taken from experiment, and ΔG^{bound}_{BA} and $\Delta G^{unbound}_{BA}$ are determined computationally.

Molecular Model. For the six α-glucose residues in αCD, standard building blocks of the GROMOS force field 53A6 were used [23]. Building blocks for the three ligands, bromobenzene (PhBr), chlorobenzene (PhCl), and toluene (PhMe), were generated based on existing Ph groups in 53A6, *e.g.*, Phe, with additional parameters for the substituents (Table S1[1])) [23][24][3]. The system was solvated in a periodic, cubic box with 2060 simple point charge (SPC) water [25] molecules and edge length of 3.99 nm, or 1056 water molecules and edge length of 3.145 nm for the complex or the free ligand in solution, respectively. The initial structure of the inclusion complex was derived from a crystal structure of αCD with 4-hydroxybenzoic acid [26]. Two kinds of perturbations exist between the three ligands. While PhBr and PhCl differ mostly in the size of the substituent, the dipole moment changes most between PhCl and PhMe. In the transformation between PhBr and PhMe, both dipole moment and the size of the substituent are perturbed. Asymmetric ligands like monosubstituted benzene derivatives can bind to αCD in two different orientations. In conformation *a* (*Fig. 1,a*), the substituent points out of the cavity into the solvent, whereas it is enclosed inside the cavity in conformation *b* (*Fig. 1,b*).

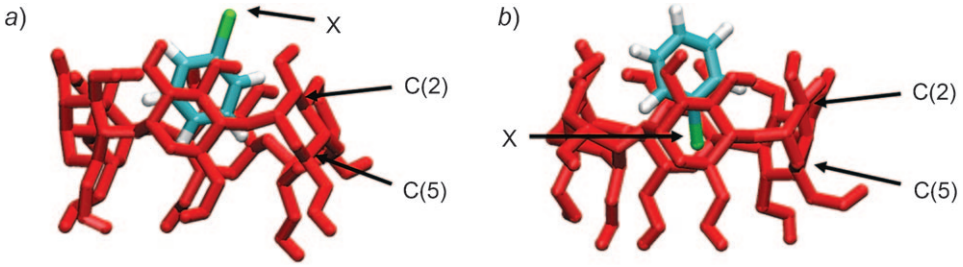

Fig. 1. a) *Monosubstituted benzene derivative bound to αCD* (red) *in conformation* a*, where the substituent X is solvent exposed.* b) *Same ligand bound to αCD* (red) *in conformation* b*, where the substituent X resides inside the cavity.* Molecular graphics generated with VMD [27].

Simulation Protocol. All simulations were performed under *NpT* conditions with the GROMOS96 package of programs [19–21] and the 53A6 GROMOS force field [23]. Simulations were carried out at three different temperatures, 250, 300, and 350 K, where for each temperature an equilibration/thermalization of a total length of 200 ps was applied. The temperature was kept to a reference value by weak coupling to a temperature bath with a relaxation time $\tau = 0.1$ ps [28], and the pressure was maintained at 1.013 bar (1 atm) by the same type of algorithm using $\tau = 0.5$ ps and an isothermal compressibility of $45.75 \cdot 10^{-5}$ kJ mol^{-1} nm^{-3}. For the nonbonded interactions, a twin-range method was used with cutoff radii of 0.8 nm (short-range) and 1.4 nm (long-range). Outside the long-range cutoff, a reaction field correction [29] with a relative dielectric permittivity $\varepsilon = 66.6$ [30] was applied. Bond lengths were constrained to minimum-energy values with SHAKE [31], allowing an integration time step of 2 fs. The center of mass motion was removed every 2 ps. Configurations of

[1]) Supplementary material is available upon request from the authors.

the system were saved every 0.5 ps. The systems were simulated at equilibrium for 5 ns. In TI, 1-ns simulations were performed at 21 equally spaced λ values between 0 and 1, where the first 100 ps were considered as equilibration and discarded for analysis. For positional restraining of the host, a force constant of $2.5 \cdot 10^4$ kJ mol^{-1} nm^{-2} was used. Unbiased simulations starting with either orientation of the ligand in the cavity resulted in preferred sampling of conformation *b*. For the calculation of ΔG_{BA} of conformation *b*, the corresponding frames were extracted from the unbiased trajectories. Simulations of conformation *a* were performed by applying distance restraints between the substituent X (X = Cl, Br, or Me) of the ligand and the C(5)-atoms of the glucose units of αCD, and between H_7 of the ligand, the H-atom opposite to the X atom, and the C(5)-atoms of the glucose units, respectively (*Fig. 1*). A force constant of 250 kJ mol^{-1} nm^{-2} was used.

Analysis. All analyses (energies, free energies, dipole moments) were performed using the tools of the GROMOS96 simulation software [19]. The time series of values of the different Hamiltonian components and of their derivatives with respect to λ were extracted from the simulation trajectories at each λ value. Errors on the corresponding averages were obtained using block averaging [32]. Polynomial interpolation was used to calculate the free-energy differences ΔG.

Results and Discussion. – *Changes in Temperature and Host Restraining.* TI Simulations of the three ligands in solution and bound to αCD were performed at 250, 300, and 350 K. Each transformation was carried out in both directions, *i.e.*, from ligand A to ligand B, and from ligand B to ligand A. In the simulations of the complex, the host was either unrestrained or positionally restrained to estimate the entropic contribution of its motion to binding. The absolute free-energy differences of all three sets of simulations are shown in *Fig. 2*. The absolute values were taken for better comparison between the transformation directions. ΔG_{BA} has a positive sign for the transformation from PhBr to PhCl and to PhMe, respectively, as well as from PhCl to PhMe. For the corresponding backward transformations, ΔG_{BA} has a negative sign. The hysteresis between forward and backward directions is found largest for the largest perturbation (PhBr to PhMe) in both the bound and the unbound state (*Fig. 2*, *a*–*c*). An effect of the temperature could only be observed for the dipole perturbations (PhBr to PhMe, and PhCl to PhMe) of the free ligands in solution. Water is highly entropic, and ΔS in these transformations comes from water around the substituent, which gains motional freedom with decreasing dipole moment of the unbound ligand. This is not the case when the ligand is bound in the cavity of αCD, so these free-energy differences are insensitive to temperature changes. However, overall the temperature-dependent differences in ΔG_{BA} are too small to calculate reliable entropy differences using the finite difference temperature method (*Eqn. 2*). In addition, ΔG_{BA} of the complexes is also not affected by rigidifying the host. It appears that for these inclusion complexes the flexibility of the host plays no role in binding.

Guest Orientation. In αCD complexes, asymmetric ligands like monosubstituted benzenes can bind in two different orientations, here called conformations *a* and *b* (see *Methods*). During simulations, flips between conformations *a* and *b* were rarely observed, although conformation *b* was sampled preferentially independent of the starting conformation, indicating that *b* is more stable. To further study the difference

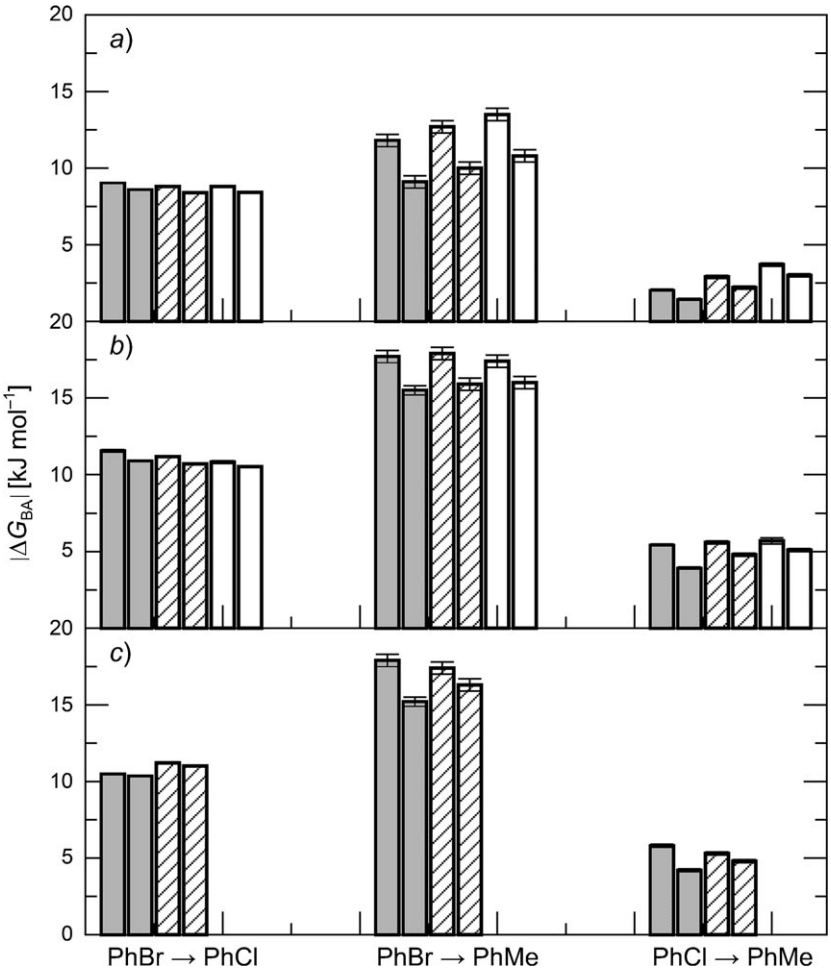

Fig. 2. *Absolute free-energy differences* $|\Delta G_{BA}|$ *of the three ligands free in solution* (*a*)*, bound to a fully flexible αCD* (*b*)*, and bound to a positionally restrained αCD* (*c*) *at 250* (grey)*, 300* (stripes)*, and 350 K* (white) *in an unbiased simulation.* TI Perturbations were performed in both directions, which are shown in the same shade.

between the two conformations, additional simulations of conformation *a* using distance restraining were performed. The free-energy differences for both conformations are shown in *Fig. 3*. From these ΔG_{BA} values, the relative binding free-energy differences $\Delta\Delta G^{BA}_{binding}$ were calculated for both conformations and compared with experimental values [10][11] (*Table 1*). The differences in ΔG_{BA} shown in *Fig. 3* are significant for all three ligands, where ΔG_{BA} is always smaller for conformation *a*. This can be explained by the type of functional group of the ligand that resides deepest inside the cavity of αCD. In conformation *b*, this group is either Br, Cl, or a Me group, while, in conformation *a*, it is always a H-atom. Thus, the change in ΔG in conformation *a* comes largely from the substituent surrounded by water, resulting in $\Delta\Delta G^{BA}_{binding}$ of

nearly zero for the transformations of the ligand in this conformational state (*Table 1*). The relative free-energy differences of binding in conformation *b* on the other hand show very good agreement with the experimental values (*Table 1*), indicating that *b* is also the dominant conformation in nature. The reason for the difference in stability of the two conformations was further investigated. Averages of the different terms of the potential energy together with the dipole moment of the ligand, the host and their scalar product are shown in *Table 2* for PhBr bound in both conformations to a positionally restrained αCD at 300 K. While, in conformation *b*, the substituent resides inside the cavity resulting in a larger nonbonded ligand–host energy term (both *Van der Waals* and electrostatic), in conformation *a*, the substituent is more accessible to solvent, as reflected by a larger ligand–solvent *Van der Waals* term $\langle E_{\mathrm{vdW}}^{\mathrm{lig-water}} \rangle$. However, the latter effect is less pronounced leading to an overall stabilization of *b* compared to *a*. Although the biggest contribution to the stabilization of conformation *b* comes from the ligand–host *Van der Waals* term $\langle E_{\mathrm{vdW}}^{\mathrm{lig-host}} \rangle$, it is also supported by the favorable antiparallel dipole–dipole arrangement shown in the negative scalar product of the dipole vectors of ligand and host $\langle \vec{\mu}_{\mathrm{lig}} \cdot \vec{\mu}_{\mathrm{host}} \rangle$. Similar, but less pronounced, results were obtained for the other two ligands (data not shown).

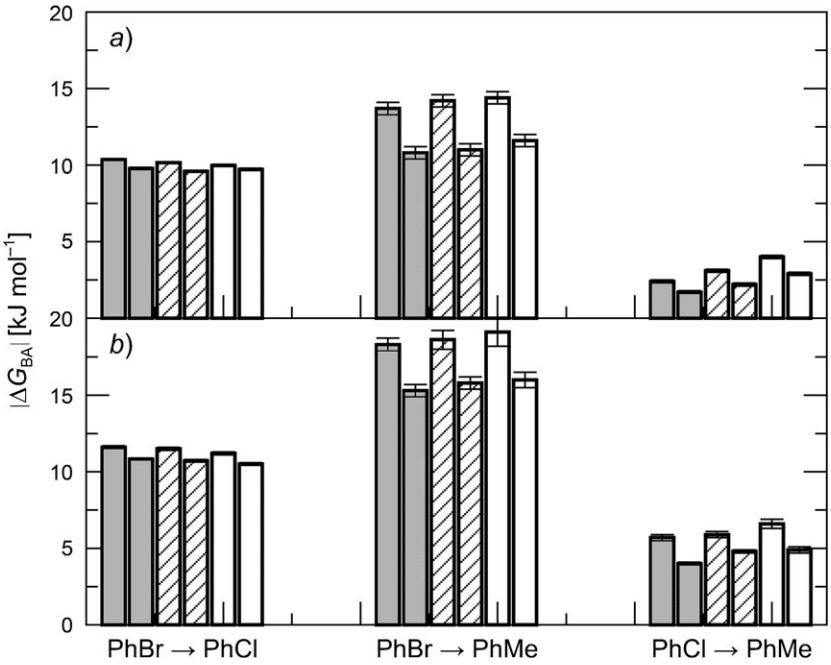

Fig. 3. *Absolute free-energy differences* $|\Delta G_{BA}|$ *of the three ligands bound to a fully flexible* α*CD at 250* (grey)*, 300* (stripes)*, and 350 K* (white) *in conformation* a (*a*) *and* b (*b*). TI Perturbations were performed in both directions, which are shown in the same shade.

Conclusions. – For this host–guest system, differences between entropic contributions to binding for different ligands play a minor role as indicated by the insensitivity

Table 1. *Experimental and Computed Relative Binding Free Energies* $\Delta\Delta G^{BA}_{binding}$ [kJ mol^{-1}] *of Fully Flexible αCD with Three Ligands BrBn, ClBn, and MeBn at 300 K for Two Conformations,* a *and* b. Computed results are shown for both TI perturbation directions. The experimental values are calculated from binding constants measured at room temperature (298 K) [10][11] using *Eqns. 3* and *4*.

Transformation	$\Delta\Delta G_{binding}$ (conf. *a*)	$\Delta\Delta G_{binding}$ (conf. *b*)	$\Delta\Delta G_{binding}$ (exper.)
PhMe → PhCl	0.205 ± 0.001	3.04 ± 0.08	2.79
PhCl → PhMe	-0.027 ± 0.002	-2.63 ± 0.02	
PhCl → PhBr	1.342 ± 0.002	2.71 ± 0.07	3.92
PhBr → PhBr	-1.213 ± 0.001	-2.30 ± 0.02	
PhMe → PhBr	1.452 ± 0.001	5.87 ± 0.20	6.71
PhBr → PhMe	-1.068 ± 0.015	-5.84 ± 0.05	

Table 2. *Averages of the Total Potential Energy* ($\langle E_{pot} \rangle$), *Bonded Term for the Complete Solute* ($\langle E^{solute}_{bnd} \rangle$), *and Nonbonded Term for the Ligand* ($\langle E^{lig}_{nb} \rangle$); *Average Dipole Moment for the Ligand* ($\langle \vec{\mu}_{lig} \rangle$), *the Host* ($\langle \vec{\mu}_{host} \rangle$), *and their Product* ($\langle \vec{\mu}_{lig} \cdot \vec{\mu}_{host} \rangle$) *for BrBn Bound to a Restrained αCD at 300 K in Both Conformations* a *and* b. The nonbonded energy term for the ligand ($\langle E^{lig}_{nb} \rangle$) is further split into its different contributions ($\langle E^{lig-host}_{vdW} \rangle$, $\langle E^{lig-water}_{vdW} \rangle$, $\langle E^{lig-lig}_{vdW} \rangle$, $\langle E^{lig-host}_{crf} \rangle$, $\langle E^{lig-water}_{crf} \rangle$, and $\langle E^{lig-lig}_{crf} \rangle$), with electrostatic interactions denoted by crf.

	Conformation *a*	Conformation *b*
$\langle E_{pot} \rangle$ [kJ mol^{-1}]	-83608 ± 219	-83632 ± 208
$\langle E^{solute}_{bnd} \rangle$ [kJ mol^{-1}]	486 ± 18	522 ± 19
$\langle E^{lig}_{nb} \rangle$ [kJ mol^{-1}]	-80 ± 8	-96 ± 8
$\langle E^{lig-host}_{vdW} \rangle$ [kJ mol^{-1}]	-43 ± 4	-55 ± 4
$\langle E^{lig-water}_{vdW} \rangle$ [kJ mol^{-1}]	-31 ± 4	-25 ± 4
$\langle E^{lig-lig}_{vdW} \rangle$ [kJ mol^{-1}]	-1.47 ± 0.03	-1.47 ± 0.03
$\langle E^{lig-host}_{crf} \rangle$ [kJ mol^{-1}]	-0.2 ± 3	-8 ± 3
$\langle E^{lig-water}_{crf} \rangle$ [kJ mol^{-1}]	-7 ± 6	-9 ± 7
$\langle E^{lig-lig}_{crf} \rangle$ [kJ mol^{-1}]	2.7 ± 0.2	2.7 ± 0.2
$\langle \vec{\mu}_{lig} \rangle$ [D]	1.4	1.4
$\langle \vec{\mu}_{host} \rangle$ [D]	12.4	12.4
$\langle \vec{\mu}_{lig} \cdot \vec{\mu}_{host} \rangle$ [D^2]	12.0	-7.2

of the free-energy differences to changes in temperature. In addition, no significant difference could be observed between perturbations using a fully flexible or a rigidified host. The reason lies, on the one hand, in the symmetry and size of the cavity of αCD, which is large enough to accommodate both PhBr and PhMe without needing structural rearrangement or affecting the strength of the host–ligand interaction. The other reason is the nature of the binding between the studied benzene derivatives and αCD, which is dominated by *Van der Waals* forces and a favorable antiparallel host–guest dipole–dipole alignment, both interactions that are rather insensitive to molecular motion inside the complex. However, guest orientation may play an important role in binding considering the different stabilities found for conformations *a* and *b*. Here, simulation can be used to interpret the experimental data at the experimentally non-observable level. While the two conformations are experimentally not distinguishable, the computed relative free energies of binding show only good agreement for conformation *b*, suggesting that this is the dominant conformation.

This work was financially supported by the *National Center of Competence in Research* (*NCCR*) *in Structural Biology*, and by grant No. 200020-121913 of the *Swiss National Science Foundation*, by grant No. 228076 of the *European Research Council*, and by grant BIO2007-62954 of the *Spanish MEC/FEDER*, which is gratefully acknowledged.

REFERENCES

[1] F. W. Lichtenthaler, S. Immel, *Liebigs Ann.* **1996**, 27.
[2] K. A. Connors, *Chem. Rev.* **1997**, *97*, 1325.
[3] A. E. Mark, S. P. van Helden, P. E. Smith, L. H. M. Janssen, W. F. van Gunsteren, *J. Am. Chem. Soc.* **1994**, *116*, 6293.
[4] M. I. El-Barghouthi, M. Schenk, M. B. Zughul, A. A. Badwan, W. F. van Gunsteren, *J. Inclusion Phenom. Macrocyclic Chem.* **2007**, *57*, 375.
[5] M. Nagarju, G. Narahari Sastry, *J. Phys. Chem. A* **2009**, *113*, 9533.
[6] P. C. Manor, W. Saenger, *J. Am. Chem. Soc.* **1974**, *96*, 3630.
[7] B. Klar, B. Hingerty, W. Saenger, *Acta Crystallogr., Sect. B* **1980**, *36*, 1154.
[8] M. Shibakami, A. Sekiya, *Carbohydr. Res.* **1994**, *260*, 169.
[9] M. V. Rekharsky, Y. Inoue, *Chem. Rev.* **1998**, *98*, 1875.
[10] L. Liu, Q.-X. Guo, *J. Phys. Chem. B* **1999**, *103*, 3461.
[11] L. Liu, W.-G. Li, Q.-X. Guo, *J. Inclusion Phenom. Macrocyclic Chem.* **1999**, *34*, 291.
[12] L. Liu, Q.-X. Guo, *J. Inclusion Phenom. Macrocyclic Chem.* **2002**, *42*, 1.
[13] W. Cai, B. Xia, X. Shao, Q.-X. Guo, B. Maigret, Z. Pan, *J. Mol. Struct. (THEOCHEM)* **2001**, *535*, 115.
[14] F. W. Lichtenthaler, S. Immel, *Starch* **1996**, *48*, 145.
[15] M. Sakurai, M. Kitagawa, H. Hoshi, Y. Inoue, R. Chûjô, *Carbohydr. Res.* **1990**, *198*, 181.
[16] E. Estrada, I. Perdomo-López, J. J. Torres-Labandeira, *J. Chem. Inf. Comput. Sci.* **2001**, *41*, 1561.
[17] J. G. Kirkwood, *J. Chem. Phys.* **1935**, *3*, 300.
[18] T. P. Straatsma, J. A. McCammon, *Annu. Rev. Phys. Chem.* **1992**, *43*, 407.
[19] W. F. van Gunsteren, S. R. Billeter, A. A. Eising, P. H. Hünenberger, P. Krüger, A. E. Mark, W. R. P. Scott, I. G. Tironi, 'Biomolecular Simulation: The GROMOS96 Manual and User Guide', vdf Hochschulverlag AG an der ETH Zürich, and BIOMOS b.v., Zürich, Groningen, 1996.
[20] W. R. P. Scott, P. H. Hünenberger, I. G. Tironi, A. E. Mark, S. R. Billeter, J. Fennen, A. E. Torda, T. Huber, P. Krüger, W. F. van Gunsteren, *J. Phys. Chem. A* **1999**, *103*, 3596.
[21] M. Christen, P. H. Hünenberger, D. Bakowies, R. Baron, R. Bürgi, D. P. Geerke, T. N. Heinz, M. A. Kastenholz, V. Kräutler, C. Oostenbrink, C. Peter, D. Trzesniak, W. F. van Gunsteren, *J. Comput. Chem.* **2005**, *26*, 1719.
[22] C. Peter, C. Oostenbrink, A. van Dorp, W. F. van Gunsteren, *J. Chem. Phys.* **2004**, *120*, 2652.
[23] C. Oostenbrink, A. Villa, A. E. Mark, W. F. van Gunsteren, *J. Comput. Chem.* **2004**, *25*, 1656.
[24] A. Almenningen, J. Brunvoll, M. V. Popik, S. V. Sokolkov, L. V. Vilkov, S. Samdal, *J. Mol. Struct.* **1985**, *127*, 85.
[25] H. J. C. Berendsen, J. P. M. Postma, W. F. van Gunsteren, J. Hermans, in 'Interaction models for water in relation to protein hydration', Reidel, Dordrecht, 1981, p. 331 – 342.
[26] K. Harata, *Bull. Chem. Soc. Jpn.* **1977**, *50*, 1416.
[27] W. Humphrey, A. Dalke, K. Schulten, *J. Mol. Graphics* **1996**, *14*, 33.
[28] H. J. C. Berendsen, J. P. M. Postma, W. F. van Gunsteren, A. Dinola, J. R. Haak, *J. Chem. Phys.* **1984**, *81*, 3684.
[29] I. G. Tironi, R. Sperb, P. E. Smith, W. F. van Gunsteren, *J. Chem. Phys.* **1995**, *102*, 5451.
[30] A. Glättli, X. Daura, W. F. van Gunsteren, *J. Chem. Phys.* **2002**, *116*, 9811.
[31] J. P. Ryckaert, G. Ciccotti, H. J. C. Berendsen, *J. Comput. Phys.* **1977**, *23*, 327.
[32] R. Friedberg, J. E. Cameron, *J. Chem. Phys.* **1970**, *52*, 6049.

Received July 1, 2010